Diffusion-controlled reactions: Mathematical formulation, variational principles, and rigorous bounds

Jacob Rubinstein
Department of Mathematics, Stanford University, Stanford, California 94305-2125

S. Torquato
Department of Mechanical and Aerospace Engineering and Department of Chemical Engineering, North Carolina State University, Raleigh, North Carolina 27695-7910

(Received 14 December 1987; accepted 21 January 1988)

This paper is concerned with the problem of predicting the effective rate constant k associated with diffusion-controlled reactions in media composed of static and reactive traps (sinks) which are generally distributed randomly throughout a region containing reactive particles. The effective equation for diffusion-controlled reactions is derived using the method of homogenization. This leads to a rigorous definition of k. General variational principles are then formulated to obtain rigorous upper and lower bounds on k. These variational principles are applied by evaluating them for three different types of admissible fields. The upper and lower bounds which result are computed for both random and periodic arrays of equisized spherical sinks.

I. INTRODUCTION

The problem of predicting the effective rate constant associated with diffusion-controlled reactions has been the subject of numerous theoretical investigations in both the physical and biological sciences and is currently attracting much attention (see the excellent review by Calef and Deutch[1] and references therein). A diffusion-controlled reaction is one in which the time for two bodies to diffuse in the same neighborhood is the rate-limiting step, the reaction time being negligible in comparison. Diffusion-controlled reactions play an important role in heterogeneous catalysis, cell metabolism, gaseous diffusion through solid, polymer chain growth kinetics, colloid or crystal growth, precipitation, fluorescence quenching, and combustion, to mention but a few examples.

We consider media composed of static and reactive traps (sinks) distributed randomly throughout a region containing reactive particles. The reactant diffuses in the trap-free region but is instantly absorbed on contact with any sink. At steady state, the rate of production σ of the diffusing species is exactly compensated by its removal by the sinks. For a particular trap or sink volume fraction ϕ_2, σ is proportional to the mean concentration field C: the proportionality constant defining the effective reaction rate constant k [see Eq. (2.12)].

The well-known Smoluchowski[2] theory deals with reactions among equisized spherical sinks of radius a at sufficiently small sink volume fractions such that interactions between sinks can be neglected; the rate constant is given by $k_s = 3\phi_2/a^2$. At higher concentrations, the reaction rate will be affected by competition between neighboring sinks. For small ϕ_2, asymptotic expansions of k for random arrays of nonoverlapping sinks (which correct the Smoluchowski result) have been derived[3,4] and are found to predict that k increases with increasing ϕ_2. The rate constant, in general, depends upon an infinite set of correlation functions which statistically characterize the medium, however; and except for specially prepared artificial media, this set of functions is never known. This explains why there are presently no exact analytical results for disordered media at arbitrary ϕ_2, even for simple models of spherical traps that are impenetrable but otherwise randomly arranged. Nonetheless, methods have been developed which enable one to estimate k for a wide range of sink concentrations; these include idealized, spatially periodic arrays of sinks,[5] approximate effective-medium theories,[6-9] random-walk techniques,[10] and variational bounds.[11,12]

This paper will focus on the study and calculation of rigorous upper and lower variational bounds on k. Rigorous bounds are useful since: (i) they may be used to test the merits of a theory, (ii) as successively more microstructural information is included, the bounds (generally) become progressively narrower, and (iii) one of the bounds can typically provide a relatively good estimate of the effective property, for a wide range of volume fractions, even when the reciprocal bound diverges from it.[13,14] There are three basic steps involved in obtaining variational bounds on effective properties:

(1) defining the effective property in terms of some functional;
(2) formulating an appropriate variational (extremum) principle for this functional;
(3) and constructing trial fields which conform with the variational principle (i.e., admissible fields).

Prager and his co-workers[15] pioneered the use of variational principles to establish bounds on effective transport properties of random media. In the present context of diffusion-controlled reactions, Reck and Prager[11] derived *three-point* lower bounds on k for random beds of spheres. (By "n-point bounds" we mean bounds that involve up to n-point correlation function information). The same authors[11] also obtained a general *two-point* upper bound on k. Doi[12] derived a general two-point lower bound on the rate constant involving different two-point correlation functions.

In Sec. II, we derive the effective equation for diffusion-

 0021-9606/88/106372-09$02.10

controlled reactions using the method of homogenization. This provides a rigorous definition of k. We then rewrite k in terms of an energy functional. In Sec. III we employ this functional to formulate rigorous upper and lower bounds on the rate constant. This formulation is new. In Sec. IV we apply the variational principles by evaluating them for three different types of admissible fields. The bounds so obtained are computed for specific microstructures. This is followed by a discussion in Sec. V.

II. MATHEMATICAL FORMULATION

A. Derivation of the effective equations using the method of homogenization

The random medium is a domain of space $\mathscr{V}(\omega)\in\mathbb{R}^3$ (where the realization ω is taken from some probability space Ω) of volume V which is composed of two regions: the trap-free region $\mathscr{V}_1$ of volume fraction ϕ_1 and the trap (sink) region $\mathscr{V}_2$ of volume fraction ϕ_2. Let $\partial\mathscr{V}$ denote the surface between $\mathscr{V}_1$ and $\mathscr{V}_2$. The characteristic function $I(\mathbf{x},\omega)$ of the trap-free region $\mathscr{V}_1(\omega)$ is defined by

$$I(\mathbf{x},\omega)=\begin{cases}1, & \mathbf{x}\in\mathscr{V}_1(\omega)\\ 0, & \mathbf{x}\in\mathscr{V}_2(\omega)\end{cases}. \tag{2.1}$$

We denote by $c(\mathbf{x})$ the concentration of the reactive particles which diffuse and are being created in $\mathscr{V}_1$, but instantaneously reacts on $\partial\mathscr{V}$:

$$D\Delta c=-\sigma \quad \text{in } \mathscr{V}_1, \tag{2.2}$$

$$c=0 \quad \text{on } \partial\mathscr{V}. \tag{2.3}$$

In Eq. (2.2), D is the diffusion coefficient of the reactive particles in $\mathscr{V}_1$ and Δ is the Laplacian operator. Equation (2.2) states that the rate of production σ of the diffusing species is exactly compensated by its removal by the traps.

We assume that the random medium has a microscopic length scale l which is small compared to a typical macroscopic length scale L. Therefore, there is a small parameter $\epsilon=l/L$ associated with rapid fluctuations in the structure of $\mathscr{V}_1(\omega)$, and we assume that the concentration c depends on two scales: a slow scale $\mathbf{x}$ and a fast scale $\mathbf{y}=\mathbf{x}/\epsilon$,[16] i.e.,

$$D\Delta c(\mathbf{x},\mathbf{y},\omega)=-\sigma(\mathbf{x}) \quad \text{in } \mathscr{V}_1^{\epsilon}(\omega), \tag{2.4}$$

$$c(\mathbf{x},\mathbf{y},\omega)=0 \quad \text{on } \partial\mathscr{V}^{\epsilon}(\omega). \tag{2.5}$$

Performing a multiscale expansion

$$c=\epsilon^2 c_0+\epsilon^3 c_1+\cdots, \tag{2.6}$$

$$\Delta=\frac{1}{\epsilon^2}\Delta_y+\frac{2}{\epsilon}\nabla_x\cdot\nabla_y+\Delta_x, \tag{2.7}$$

one finds that the leading order equation [after substituting Eqs. (2.6) and (2.7) into Eq. (2.4)] is given by

$$D\Delta_y c_0(\mathbf{x},\mathbf{y},\omega)=-\sigma(\mathbf{x}). \tag{2.8}$$

Hence, we can write

$$c_0(\mathbf{x},\mathbf{y},\omega)=D^{-1}\sigma(\mathbf{x})w(\mathbf{y},\omega), \tag{2.9}$$

where the auxiliary function w is defined through

$$\Delta_y w(\mathbf{y},\omega)=-1 \quad \text{in } \mathscr{V}_1(\omega), \tag{2.10}$$

$$w(\mathbf{y},\omega)=0 \quad \text{on } \partial\mathscr{V}(\omega), \tag{2.11}$$

and we extend w in the trap region $\mathscr{V}_2(\omega)$ to be zero. We now add the assumption that the medium is locally (i.e., on scale) stationary. Then the ensemble average of any function $g(\mathbf{x},\mathbf{y},\omega)$ is a simple function of $\mathbf{x}$ only, i.e.,

$$\langle g(\mathbf{x},\mathbf{y},\omega)\rangle=\langle g\rangle(\mathbf{x}),$$

where $\langle\cdot\rangle$ denotes an ensemble average. *Homogenization* refers to averaging on the fast scale.[16] Averaging Eq. (2.9) then yields

$$\sigma(\mathbf{x})=kDC(\mathbf{x}), \tag{2.12}$$

where the constant k is the reaction rate constant[17] given by

$$k^{-1}=\langle w(\mathbf{y},\omega)\rangle=\langle w(\mathbf{y},\omega)I(\mathbf{y},\omega)\rangle \tag{2.13}$$

and

$$C(\mathbf{x})=\langle c_0\rangle(\mathbf{x}). \tag{2.14}$$

To our knowledge, this is the first time that the effective equation which defines the rate constant has been derived using the method of homogenization.

B. Energy characterization of the rate constant

We now rewrite k in terms of an energy functional.

1. Proposition 1

$$k^{-1}=\langle\nabla w(\mathbf{y},\omega)\cdot\nabla w(\mathbf{y},\omega)I(\mathbf{y},\omega)\rangle. \tag{2.15}$$

2. Proof

Let V_R be a large ball of radius R centered at the origin. Then we have

$$\begin{aligned}\langle w\Delta wI\rangle&=\langle w\Delta w\rangle\\ &=\frac{1}{V_R}\int\langle w\Delta w\rangle d\mathbf{y}=\left\langle\frac{1}{V_R}\int_{V_R}w\Delta w\,d\mathbf{y}\right\rangle\\ &=\left\langle\frac{-1}{V_R}\int_{V_R}\nabla w\cdot\nabla w\,d\mathbf{y}\right\rangle\\ &\quad+\left\langle\frac{1}{V_R}\int_{\partial V_R}w\frac{\partial w}{\partial n}d\mathbf{y}\right\rangle\\ &\quad+\left\langle\frac{1}{V_R}\int_{\partial\gamma}w\frac{\partial w}{\partial n}d\mathbf{y}\right\rangle\\ &=-\langle\nabla w\cdot\nabla w\rangle+\frac{1}{V_R}\int_{\partial V_R}\left\langle w\frac{\partial w}{\partial n}\right\rangle d\mathbf{y}.\end{aligned}$$

The last integral of the second line vanishes identically because of condition (2.11). The quantity ∂V_R denotes the trap-free part of the surface of the large ball. Letting $R\to\infty$, we find

$$\langle w\Delta w\rangle=-\langle\nabla w\cdot\nabla w\rangle$$

and since by Eq. (2.13),

$$k^{-1}=\langle wI\rangle=-\langle w\Delta w\rangle$$

the proof is complete.

3. Remark

In subsequent analysis, we shall exploit the stationarity of the medium to derive other identitites (by the same method employed here) without spelling out the details.

III. VARIATIONAL BOUNDS

We consider deriving upper and lower bounds on the rate constant k using variational principles. To do so, we modify Eq. (2.10) slightly by introducing the function $v = \gamma w$. The quantity v solves

$$\Delta_y v(\mathbf{y},\omega) = -\gamma \quad \text{in } \mathscr{V}_1(\omega), \tag{3.1}$$

$$v(\mathbf{y},\omega) = 0 \quad \text{on } \partial\mathscr{V}(\omega) \text{ and in } \mathscr{V}_2(\omega). \tag{3.2}$$

Then k satisfies

$$\gamma = k\langle v\rangle = k\langle vI\rangle. \tag{3.3}$$

A. Lower bound

Let A be the class of functions u defined by the set

$$A = \{\text{smooth, stationary } u(\mathbf{y},\omega);\ \Delta u = -\gamma \text{ in } \nu_1\}. \tag{3.4}$$

Then k is bounded from below by

$$k \geqslant \frac{\gamma^2}{\langle \nabla u\cdot\nabla uI\rangle} \quad \forall u\in A. \tag{3.5}$$

1. Proof

From Proposition 1, it follows that

$$k = \frac{\gamma^2}{\langle \nabla v\cdot\nabla vI\rangle}. \tag{3.6}$$

Let now $u\in A$. Then writing $u = v + g$, we get

$$\langle \nabla u\cdot\nabla uI\rangle = \langle \nabla v\cdot\nabla vI\rangle + \langle \nabla g\cdot\nabla gI\rangle + 2\langle \nabla v\cdot\nabla gI\rangle.$$

But $\Delta g = 0$ implies $\langle \nabla v\cdot\nabla gI\rangle = 0$, so that

$$\langle \nabla u\cdot\nabla uI\rangle \geqslant \langle \nabla v\cdot\nabla vI\rangle.$$

This last inequality combined with Eq. (3.6) leads to Eq. (3.5): the equality sign applying when u is the exact solution to Eqs. (3.1) and (3.2), i.e., $u = v$. The lower bound (3.5) is new.

B. Upper bound

Let B be the class of functions u defined by the set

$$B = \{\text{smooth, stationary } u(\mathbf{y},\omega);\ u = 0 \text{ on } \partial\mathscr{V}_1 \text{ and } \langle uI\rangle = \langle vI\rangle\}. \tag{3.7}$$

Then k is bounded from above by

$$k \leqslant \frac{\langle \nabla u\cdot\nabla uI\rangle}{\langle v\rangle^2} \quad \forall u\in B. \tag{3.8}$$

1. Proof

Eliminating γ from Eqs. (3.1) and (3.3), and applying Proposition 1 yields

$$k = \frac{\langle \nabla v\cdot\nabla vI\rangle}{\langle vI\rangle^2}. \tag{3.9}$$

Consider $u\in B$ and define $u = v + g$. Then

$$\langle \nabla u\cdot\nabla uI\rangle = \langle \nabla v\cdot\nabla vI\rangle + \langle \nabla g\cdot\nabla gI\rangle + 2\langle \nabla v\cdot\nabla gI\rangle.$$

Integrating by parts as in the proof of Proposition 1, we find

$$\langle \nabla v\cdot\nabla gI\rangle = \gamma\langle gI\rangle = 0$$

since $\langle gI\rangle = \langle uI\rangle - \langle vI\rangle$, so that again $\langle \nabla u\cdot\nabla uI\rangle \geqslant \langle \nabla v\cdot\nabla vI\rangle$. This inequality together with Eq. (3.9) proves upper bound (3.8) which is new.

2. Remark

In certain instances it may be advantageous to use bounds that are cruder than Eqs. (3.5) and (3.8), namely

$$k \geqslant \frac{\gamma^2}{\langle \nabla u\cdot\nabla u\rangle} \quad \forall u\in A, \tag{3.10}$$

$$k \leqslant \frac{\langle \nabla u\cdot\nabla u\rangle}{\langle v\rangle^2} \quad \forall u\in B. \tag{3.11}$$

The reason for this is that computation of $\langle \nabla u\cdot\nabla u\rangle$ ($\geqslant \langle \nabla u\cdot\nabla uI\rangle$) involves less detailed microstructural information (i.e., lower order correlation functions) than the evaluation of $\langle \nabla u\cdot\nabla uI\rangle$.

C. Volume-average approach

Thus far we have used an ensemble-average approach. An alternative derivation is possible by considering averages over a large but finite volume and then allowing the volume to expand to infinity. Let V be a large domain (in which we ultimately take the limit $V\to\mathbb{R}^3$), ∂V be the surface of the domain, and consider

$$\Delta v = -\gamma \quad \text{in } \mathscr{V}_1, \tag{3.12}$$

$$v = 0 \quad \text{on } \partial\mathscr{V}, \tag{3.13}$$

$$\frac{\partial v}{\partial n} = 0 \quad \text{on } \partial V. \tag{3.14}$$

Next we define the volume average

$$\bar{v} = \frac{1}{V}\int_{\mathscr{V}_1} v\, dV \tag{3.15}$$

and the reaction rate constant

$$k\bar{v} = \gamma. \tag{3.16}$$

The following bounds hold for k.

D. Lower bound

$$k \geqslant \frac{\gamma^2}{\overline{\nabla u\cdot\nabla u}} \quad \forall u\in A_1, \tag{3.17}$$

$$A_1 = \left\{u;\ \Delta u = -\gamma \text{ in } \mathscr{V}_1, \frac{\partial u}{\partial n} = 0 \text{ on } \partial V\right\}. \tag{3.18}$$

E. Upper bound

$$k \leqslant \frac{\overline{\nabla u\cdot\nabla u}}{\bar{v}^2} \quad \forall u\in B_1, \tag{3.19}$$

$$B_1 = \{u;\ u = 0 \text{ on } \partial\mathscr{V},\ \bar{u} = \bar{v}\}. \tag{3.20}$$

The bounds (3.17) and (3.19) may be proved in a similar fashion to the previously derived ensemble-averaged bounds and hence the proofs are not presented here. Note the volume averages of Eqs. (3.17) and (3.19) are defined in the same sense as Eq. (3.15) (i.e., the domain of integration is the trap-free region $\mathscr{V}_1$) and it is implicit that the limit $V\to\infty$ is taken.

IV. EXAMPLES OF TRIAL FIELDS AND BOUNDS

In order to apply the rigorous bounds on k (derived in the previous section) for models of random media, we must choose admissible trial fields, substitute such trials fields into the bounds, and then perform the necessary averaging.

A. Interfacial-surface lower bounds

We rederive a lower bound obtained by Doi[12] using our variational lower bound (3.10). Our derivation is different than his, and in fact we show his bound corresponds to a special choice of a trial field in the set A, Eq. (3.4), and not to a new variational principle as Doi stated. Specifically, we choose

$$u_1(\mathbf{y},\omega) = \gamma\left[\int_{\mathscr{V}_1} G(\mathbf{y}-\mathbf{x})d\mathbf{x} - \int_{\partial\mathscr{V}} G(\mathbf{y}-\mathbf{x})\xi(\mathbf{x})d\mathbf{x}\right], \tag{4.1}$$

where

$$G(\mathbf{x},\mathbf{y}) = \frac{1}{4\pi}\frac{1}{|\mathbf{x}-\mathbf{y}|} \tag{4.2}$$

is the Green's function of the Laplacian operator Δ. The quantity $\xi(\mathbf{x})$ is an arbitrary function which is defined on the interfacial surface $\partial\mathscr{V}$. Accordingly, we refer to this procedure as the interfacial-surface approach.

To get a lower bound we compute the ensemble average

$$\langle \nabla u_1 \cdot \nabla u_1 \rangle = \gamma^2\left[\left\langle \int_{\mathscr{V}_1}\int_{\mathscr{V}_1} \nabla G(\mathbf{y}-\mathbf{x})\cdot\nabla G(\mathbf{y}-\mathbf{z})d\mathbf{x}\,d\mathbf{z}\right\rangle - 2\left\langle \int_{\mathscr{V}_1}\int_{\partial\mathscr{V}} \nabla G(\mathbf{y}-\mathbf{x})\cdot\nabla G(\mathbf{y}-\mathbf{z})\xi(\mathbf{x})d\mathbf{x}\,d\mathbf{z}\right\rangle + \left\langle \int_{\partial\mathscr{V}}\int_{\partial\mathscr{V}} \nabla G(\mathbf{y}-\mathbf{x})\cdot\nabla G(\mathbf{y}-\mathbf{z})\xi(\mathbf{x})\xi(\mathbf{z})d\mathbf{x}\,d\mathbf{z}\right\rangle\right]. \tag{4.3}$$

In carrying out the averages of Eq. (4.3) we will make use of the following two-point correlation functions:

$$F_{vv}(\mathbf{r}) = \langle I(\mathbf{y})I(\mathbf{y}+\mathbf{r})\rangle, \tag{4.4}$$

$$F_{sv}(\mathbf{r}) = \langle |\nabla I(\mathbf{y})| I(\mathbf{y}+\mathbf{r})\rangle, \tag{4.5}$$

$$F_{ss}(\mathbf{r}) = \langle |\nabla I(\mathbf{y})||\nabla I(\mathbf{y}+\mathbf{r})|\rangle. \tag{4.6}$$

These functions are called void–void, surface–void, and surface–surface correlation functions, respectively. These correlation functions and their generalizations (e.g., F_{ssv},F_{sss}, etc.) have been extensively studied by Torquato.[14] We are free to choose $\xi(\mathbf{x})$ subject to the constraint that the right-hand side of Eq. (4.3) is finite. For simplicity, we choose ξ to be a constant ξ_0. Then Eqs. (3.5) and (4.3) imply

$$k \geqslant \left[\int G(\mathbf{r})\{\xi_0^2 F_{ss}(\mathbf{r}) - 2\xi_0 F_{sv}(\mathbf{r}) + F_{vv}(\mathbf{r})\}\,d\mathbf{r}\right]^{-1}. \tag{4.7}$$

The asymptotic behavior as $|\mathbf{r}|\to\infty$ of the correlation functions in Eq. (4.7) is well known:

$$F_{ss}(\mathbf{r})\to s^2, \quad F_{sv}(\mathbf{r})\to s\phi_1, \quad F_{vv}(\mathbf{r})\to\phi_1^2, \tag{4.8}$$

where $\phi_1 = \langle I(\mathbf{y})\rangle$ is the expected volume fraction of the trap-free region $\mathscr{V}_1$ (porosity) and $s = \langle |\nabla I(\mathbf{y})|\rangle$ is the expected area of the interface $\partial\mathscr{V}$ per unit volume (specific surface). Hence, the only choice of ξ_0 for which the integral of Eq. (4.7) exists is

$$\xi_0 = \phi_1/s. \tag{4.9}$$

Therefore,

$$k \geqslant \left\{\int \frac{1}{4\pi r}\left[\frac{\phi_1^2}{s^2}F_{ss}(\mathbf{r}) - \frac{2\phi_1}{s}F_{sv}(\mathbf{r}) + F_{vv}(\mathbf{r})\right]d\mathbf{r}\right\}^{-1}. \tag{4.10}$$

The two-point lower bound (4.10) was first derived by Doi.[12] The derivation of Eq. (4.10) presented here, however, is new. The trial field Eq. (4.1) corresponds to a special choice of admissible fields in the set A, Eq. (3.4), for the minimum energy principle (3.5) and not to a new variational principle as Doi claimed. We further remark that Doi made the choice (4.9) after "optimizing" Eq. (4.7) over all possible ξ_0. However, as we have argued, any other choice for ξ_0 will provide a trivial bound (namely, $k\geqslant 0$), so there is actually no room for optimization.

B. Evaluation of the interfacial-surface lower bound for distributions of spherical traps

We now evaluate the lower bound (4.10) for an isotropic distribution of equisized spherical sinks of radius a. The sinks are distributed with an arbitrary degree of impenetrability λ. The impenetrability parameter λ varies continuously between zero (in the case where the sphere centers are randomly centered, i.e., "fully penetrable" spheres) and unity (in the instance of totally impenetrable spheres). Two examples of such interpenetrable-sphere models are the permeable-sphere (PS)[18] and penetrable-concentric-shell (PCS)[19] models. In the PS model, the spheres are assumed to be (structurally) noninteracting when nonintersecting, with a probability of intersection given by a radial distribution function $g(r) = 1-\lambda$, independent of the interparticle separation distance r when $r<2a$. In the PCS model, spherical particles of radius a are randomly distributed subject to the condition of a mutually impenetrable core region of radius λa, $0\leqslant\lambda\leqslant 1$. Each sphere may be thought of as being composed of an impenetrable core of radius λa, encompassed by a perfectly penetrable concentric shell of thickness $(1-\lambda)a$. In Figs. 1 and 2 computer-generated realizations of two-dimensional distributions of disks in the PS and PCS models are shown. In the former model, two particle centers may lie arbitrarily close to one another such that the probability of overlap is $1-\lambda$; in the latter model no two particle centers may lie closer than the distance $2a\lambda$.

Note that for fully penetrable spheres ($\lambda = 0$), the volume fraction of the trap-free region is $\phi_1 = \exp[-\eta]$ (where $\eta = 4\pi a^3\rho/3$ is a reduced density) and the specific surface is $s = 3\eta\phi_1/a$.[14] In the opposite limit of totally impenetrable spheres ($\lambda = 1$), $\phi_1 = 1-\eta$ (or, $\phi_2 = \eta$) and $s = 3\phi_2/a$. These results indicate that $\phi_2(\lambda=1)\geqslant\phi_2(\lambda=0)$ and $s(\lambda=1)\geqslant s(\lambda=0)$: the equa-

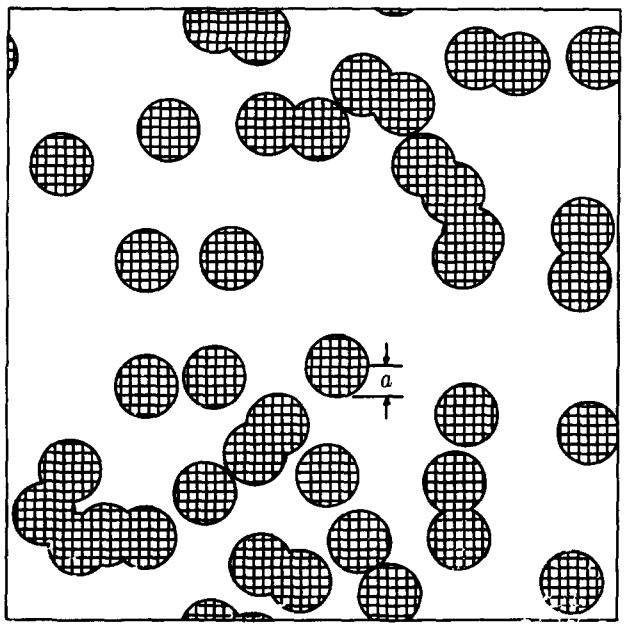

FIG. 1. A computer-generated realization of a distribution of disks of radius a (shaded region) in the PS model (Ref. 18). Here the impenetrability parameter $\lambda = 0.5$ and the sink volume fraction $\phi_2 = 0.3$.

lity sign applying in the dilute limit (i.e., through first order in η).

Utilizing the series representation of the two-point correlation functions of Eq. (4.10) in terms of the n-particle probability densities[14] [defined by Eq. (4.17)], we compute Eq. (4.10) through second order in the sink volume fraction ϕ_2 in the PS model and find

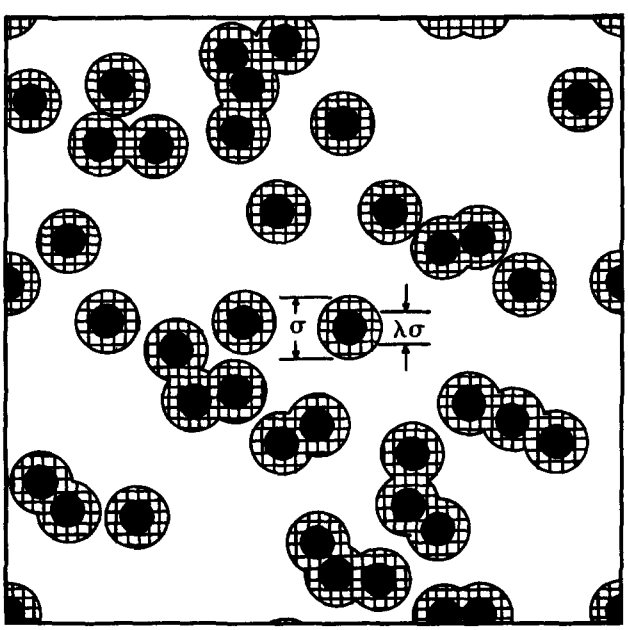

FIG. 2. A computer-generated realization of a distribution of disks of radius $a = \sigma/2$ (shaded region) in the PCS model (Ref. 19). The disks have an impenetrable core of diameter $\lambda\sigma$ indicated by the smaller, black circular region. Here $\lambda = 0.5$ and $\phi_2 = 0.3$.

$$k/k_s \geqslant 1 + K_2\phi_2 + O(\phi_2^2), \tag{4.11}$$

where

$$K_2 = \tfrac{15}{8} + \tfrac{25}{8}\lambda \tag{4.12}$$

and

$$k_s = \frac{3\phi_2}{a^2}. \tag{4.13}$$

Note that through first order in ϕ_2, the bound gives the exact Smoluchowski result k_s. The next term accounts for interactions between pairs of sinks; as the impenetrability parameter λ increases, the second-order coefficient K_2 increases, as expected, since the surface area available for reaction increases.

We also evaluate K_2 in the PCS model for $0 < \lambda < 1$; in the extreme limits $\lambda = 0$ and $\lambda = 1$, the results are of course the same as that for the PS model, Eq. (4.12). For intermediate values of λ, K_2 had to be computed numerically: for $\lambda = 0.2$, 0.4, 0.6, and 0.8, $K_2 = 1.88$, 1.96, 2.30, and 3.19, respectively. Therefore, the second-order coefficient in the PCS model is always less than the corresponding value in the PS model for intermediate values of the impenetrability parameter.

It is of interest to compare our low-density bounds to a low-density expansion of k for impenetrable spherical sinks ($\lambda = 1$) recently derived by Mattern and Felderhof[4]:

$$\frac{k}{k_s} = 1 + \sqrt{3}\phi_2^{1/2} - 3E_1(6\sqrt{3\phi_2})\phi_2 + 5.7321\phi_2 + \text{h.o.t.} \tag{4.14}$$

Here E_1 is the exponential integral. A notable feature of this asymptotic expansion is the nonanalytic dependence on ϕ_2. The expansion (4.14) predicts an $O(\phi_2^{1/2})$ correction to the Smoluchowski result as opposed to an $O(\phi_2)$ correction from the bound (4.11). This leading order correction has been obtained by others.[3,6–10] The nonanalyticity is a direct consequence of diffusional screening effects. We note that at $\phi_2 = 0.01$, the expansion predicts $k/k_s = 1.20$, whereas the lower bound (4.11) for $\lambda = 1$ gives $k/k_s > 1.05$. Clearly, for dilute conditions, the $\phi_2^{1/2}$ term is the dominant term. It is difficult to construct trial fields which incorporate screening and simultaneously satisfy the conditions of the set A, Eq. (3.4). Means of obtaining nonanalytic bounds shall be dealt with in a future work.

We remark that lower bound (4.10) has been numerically computed to all orders in ϕ_2 for fully penetrable spherical sinks[12] and for totally impenetrable sinks.[20,21] For subsequent discussion, we plot these results in Fig. 3. Note that effective-medium theories which attempt to approximate k (for impenetrable sinks) for arbitrary sink concentrations,[6,9] while giving an order $\phi_2^{1/2}$ correction to the Smoluchowski result, fall below (i.e., violate) the lower bound of Fig. 3 for impenetrable sinks at moderate values of ϕ_2.[9,20,21]

C. Multiple-scattering lower bounds

If the medium is composed of a distribution of inclusions, we can construct trial fields which are based on the solutions for scattering from a single inclusion, pairs of inclusions, etc. Accordingly, we refer to bounds so obtained as

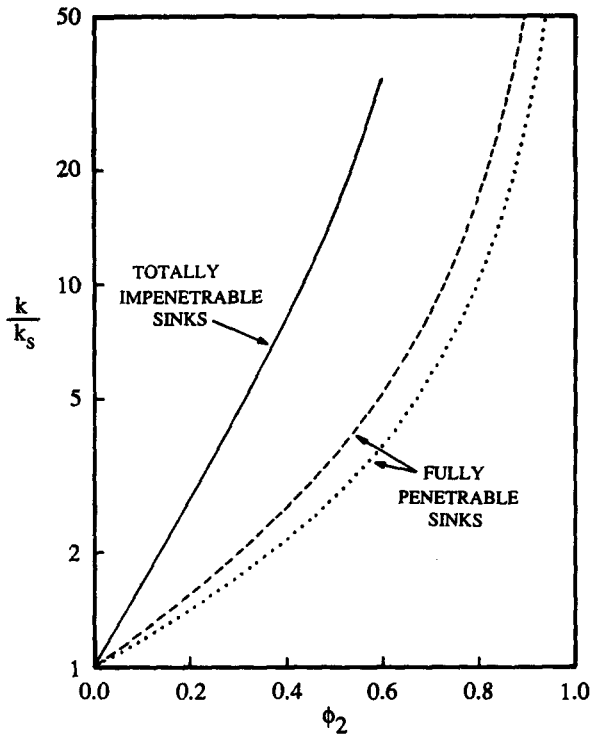

FIG. 3. Lower bounds on the reduced rate constant k/k_s vs the sink volume fraction ϕ_2. Solid (—) line is two-point bound (4.10) for totally impenetrable spherical sinks ($\lambda = 1$) computed in Ref. 20. Dashed (---) line is two-point bound (4.10) for fully penetrable spherical sinks ($\lambda = 0$) computed in Ref. 12. Dotted (···) line is our three-point bound (4.29) for fully penetrable sinks.

multiple-scattering bounds. For the case of a distribution of N identical spheres of radius a, we can construct the following single-scatterer trial field:

$$u_1 = \gamma\left[\int G(\mathbf{y}-\mathbf{x})d\mathbf{x} - \alpha\sum_{i=1}^{N} G(\mathbf{y}-\mathbf{r}_i)e(|\mathbf{y}-\mathbf{r}_i|)\right], \tag{4.15}$$

where

$$e(r) = \begin{cases} 0, & r<a \\ 1, & r>a \end{cases} \tag{4.16}$$

is the characteristic function of the exterior of a single sphere, $\mathbf{r}_i$ is the position of the ith sphere, and α is a parameter. It turns out that the only choice for which the energy $\langle \nabla u_2 \cdot \nabla u_2 I\rangle$ is finite, is $\alpha = 1/\rho$ (where it is to be recalled that ρ is the number density of the spheres). Trial functions of this type have been employed recently in the problems of conduction in composite media[22] and in viscous flow in porous media.[23]

Before computing $\langle \nabla u_2 \cdot \nabla u_2 I\rangle$, we introduce the following statistical distribution functions for the random medium:

$$\rho_n(\mathbf{r}^n) = \frac{N!}{(N-n)!}\int P_N(\mathbf{r}^N)d\mathbf{r}_{n+1}\cdots d\mathbf{r}_N, \tag{4.17}$$

$$G_n(\mathbf{x};\mathbf{r}^q) = \frac{N!}{(N-q)!} \times \int I(\mathbf{x})P_N(\mathbf{r}^N)d\mathbf{r}_{q+1}\cdots d\mathbf{r}_N,\ n = 1+q. \tag{4.18}$$

Here $P_N(\mathbf{r}^N)$ is the probability density function associated with the event of finding particles 1,..., N with configuration $\mathbf{r}^N \equiv \{\mathbf{r}_1,...,\mathbf{r}_N\}$, respectively. Then $\rho_n(\mathbf{r}^n)$ is the probability density associated with finding any n particles with configuration $\mathbf{r}^n$, while $G_n(\mathbf{x};\mathbf{r}^q)$ is the correlation function associated with finding $\mathbf{x}$ in the trap-free region and any q particles with configuration $\mathbf{r}^q, n = 1+q$. The G_n have been expressed as an infinite series involving the ρ_n:[14,22]

$$G_n(\mathbf{x};\mathbf{r}^q) = \prod_{i=1}^{n} e(z_i)\sum_{k=0}^{\infty}\int \rho_{q+k}(\mathbf{r}_1,\cdots,\mathbf{r}_{q+k}) \times \prod_{j=q+1}^{q+k} m(z_j)d\mathbf{r}_j, \tag{4.19}$$

where

$$m(r) = 1 - e(r) \tag{4.20}$$

is the characteristic function of the interior of an inclusion, $\mathbf{z}_i = \mathbf{x} - \mathbf{r}_i$, and $z_i = |\mathbf{z}_i|$. The condition of stationarity (statistical homogeneity) implies than the n-particle probability density can be written as $\rho_n(\mathbf{r}^n) = \rho^n g_n(\mathbf{r}^n)$. When the mutual distances between the n particles become large, the n-particle distribution function $g_n \to 1$, assuming no long-range order. Relation (4.19) is important since it enables one to compute the G_n when the ensemble is fully specified, i.e., when the ρ_n are given. Note that the factor multiplying the infinite series of Eq. (4.19) ensures that $G_n(\mathbf{x};\mathbf{r}^q) = 0$ for any $|\mathbf{x} - \mathbf{r}_i| < a$, i.e., whenever the point $\mathbf{x}$ is contained within a sink.

We now observe that

$$\langle \nabla u_2 \cdot \nabla u_2 I\rangle = \langle \boldsymbol{\tau}\cdot\boldsymbol{\tau} I\rangle \leqslant \langle \boldsymbol{\tau}\cdot\boldsymbol{\tau}\rangle, \tag{4.21}$$

where

$$\boldsymbol{\tau} = \gamma\left[\int \nabla G(\mathbf{y}-\mathbf{x})d\mathbf{x} - \frac{1}{\rho}\sum_{i=1}^{N}\nabla G(\mathbf{y}-\mathbf{r}_i)e(|\mathbf{y}-\mathbf{r}_i|)\right]. \tag{4.22}$$

Thus, Eqs. (3.5) and (4.21) yield the following two-point lower bound:

$$k \geqslant \left[\frac{1}{\rho}\int_{z_1>a}\nabla G(\mathbf{z}_1)\cdot\nabla G(\mathbf{z}_1)d\mathbf{z}_1 + \int_{z_1>a}\int_{z_2>a} h(\mathbf{r}_{12})\nabla G(\mathbf{z}_1)\cdot\nabla G(\mathbf{z}_2)d\mathbf{z}_1\, d\mathbf{z}_2\right]^{-1}, \tag{4.23}$$

where

$$h(\mathbf{r}) = g_2(\mathbf{r}) - 1 \tag{4.24}$$

is the total pair correlation function and $\mathbf{r}_{ij} = \mathbf{r}_j - \mathbf{r}_i$. Note that the integrals of Eq. (4.23) are absolutely convergent; the second one is convergent since $h(\mathbf{r})$ tends to zero much more rapidly than r^{-3} as $r \to \infty$. In fact, the first integral in Eq. (4.23) can be evaluated explicitly and we get the following bound:

$$k \geqslant \left[\frac{1}{4\pi a\rho} + \int_{z_1>a}\int_{z_2>a} h(\mathbf{r}_{12})\nabla G(\mathbf{z}_1)\cdot\nabla G(\mathbf{z}_2)d\mathbf{z}_1\, d\mathbf{z}_2\right]^{-1}. \tag{4.25}$$

Use of Eq. (3.5) together with Eq. (4.15) yields the following three-point lower bound:

$$k \geqslant \left[\frac{1}{\rho^2} \int G_2(\mathbf{r}_1) |\nabla G(\mathbf{r}_1)|^2 d\mathbf{r}_1 + \frac{1}{\rho^2} \int \int Q_3(\mathbf{r}_1,\mathbf{r}_2) \nabla G(\mathbf{r}_1) \cdot \nabla G(\mathbf{r}_2) d\mathbf{r}_1 \, d\mathbf{r}_2 \right]^{-1}, \tag{4.26}$$

where

$$Q_3(\mathbf{r}_1,\mathbf{r}_2) = G_3(\mathbf{x};\mathbf{r}_1,\mathbf{r}_2) - \rho G_2(\mathbf{x};\mathbf{r}_1) - \rho G_2(\mathbf{x};\mathbf{r}_2) + \rho^2 \phi_1. \tag{4.27}$$

The asymptotic behavior of Q_3 for large separations[22] ensures the absolute convergence of the second integral of Eq. (4.26).

D. Evaluation of multiple-scattering lower bounds for distributions of spherical traps

Here we compute the multiple-scattering lower bounds (derived in the previous subsection) for distributions of equisized spherical traps of radius a. First consider the exact evaluation of the two- and three-point lower bounds to all orders in ϕ_2 for the case of fully penetrable spheres ($\lambda = 0$). For such a microstructure, $h(r) = 0$ for all r, and the two-point lower bound (4.23) gives

$$\frac{k}{k_s} \geqslant -\frac{\ln \phi_1}{\phi_2}. \tag{4.28}$$

Comparing Eq. (4.10) for the instance of fully penetrable spheres to Eq. (4.28) reveals that the two-point interfacial-surface bound is sharper than the two-point multiple-scattering bound through all orders in ϕ_2. For this model, the G_n described by Eq. (4.19) are trivial,[14,22] and the three-point lower bound (4.26) gives

$$\frac{k}{k_s} \geqslant \frac{-\ln \phi_1}{\phi_1 \phi_2}, \tag{4.29}$$

which is clearly a better lower bound than Eq. (4.28). Therefore, incorporation of additional statistical information in multiple-scattering-type bounds leads to progressively sharper bounds. In Fig. 3 we include lower bound (4.29). Even though Eq. (4.29) contains three-point information, it is seen (from Fig. 3) that, for the geometry of fully penetrable spheres, it is inferior to the interfacial-surface lower bound (4.10) which contains only two-point information.

This last statement will not be true for all λ, however. For example, using the low-density expansion of Eq. (4.19) for the cases $n = 2$ and $n = 3$, the three-point multiple-scattering bound yields an expansion of the form of Eq. (4.11) with

$$K_2 = \tfrac{3}{2} + \lambda(2 + \tfrac{15}{8} \ln 3), \tag{4.30}$$

in the PS model and

$$K_2 = \tfrac{3}{2} - \lambda^6 + 3\lambda^4 + \tfrac{9}{8}\lambda^2 - \tfrac{9}{8}\lambda + \tfrac{3}{8}(1 + 4\lambda^2)\ln(1 + 2\lambda). \tag{4.31}$$

Comparing Eqs. (4.30) and (4.31) to the corresponding results for the two-point interfacial-surface bounds obtained above, reveals that for a large range of λ (for $\lambda > 0.37$ in the PS model and $\lambda > 0.60$ in the PCS model) the three-point multiple-scattering bounds are sharper than the two-point interfacial-surface bounds. The reason why the former are superior to the latter for large λ is discussed in the subsequent section. Finally, we remark that the behavior of the lower bounds at low densities gives an indication of how the bounds will behave at all sink concentrations.[22,23] For example, for totally impenetrable sinks ($\lambda = 1$), the three-point bound (4.26) should be sharper than the two-point bound (4.10) for all ϕ_2.

E. Security-spheres upper bounds

The construction of a trial concentration field u for the upper bounds (3.8) or (3.19) is more problematical than the lower bound because of the condition that $u = 0$ on the interface $\partial\mathscr{V}$. Consider constructing a trial field for a distribution of N identical spheres of radius a. Let the distance between the ith sphere and it nearest neighbor be denoted by $2b_i$. In addition we assume $b_i > a \ \forall i$. It is more convenient here to use the expanding-volume formulation (3.19). A trial field $\psi \in B_1$ [where B_1 is given Eq. (3.20)] is chosen as follows: for every sphere i we consider the domain defined by itself and a concentric 'security' sphere of radius b_i. In that domain we solve

$$\begin{aligned} &\Delta\psi_i(\mathbf{x}) = 0 \quad \text{in } a < |\mathbf{x} - \mathbf{r}_i| < b_i, \\ &\psi_i = 0 \quad \text{on } |\mathbf{x} - \mathbf{r}_i| = a, \\ &\psi_i = \zeta \quad \text{on } |\mathbf{x} - \mathbf{r}_i| = b_i. \end{aligned} \tag{4.32}$$

The trial field ψ is chosen to be equal to ψ_i in the ith security shell and to be ζ elsewhere. Finally, we choose ζ such that $\bar{\psi} = \bar{v}$. The security-spheres method has been employed in the related problems of bounds on the viscosity of suspensions[24] and the permeability of porous media.[25]

Solving Eq. (4.32) and eliminating ζ in Eq. (3.19) yields

$$\frac{k}{k_s} \leqslant \frac{1}{N} \sum_{i=1}^{N} d(\beta_i) \Big/ \left[1 - \frac{\phi_2}{2} \frac{1}{N} \sum_{i=1}^{N} f(\beta_i) \right]^2, \tag{4.34}$$

$$d(x) = \frac{x}{x-1}, \tag{4.35}$$

$$f(x) = x(1 + x), \tag{4.36}$$

where $\beta_i = b_i/a$ and $\phi_2 = \eta = 4\pi a^3 \rho/3$. In the lower bound (4.34), it is understood that the "thermodynamic" limit is taken (i.e., $N \to \infty$, $V \to \infty$, such that $\rho = N/V$ is fixed). Using the law of large numbers, we can write Eq. (4.34) as

$$\frac{k}{k_s} < a \int_1^\infty d(\beta) H(a\beta) d\beta \Big/ \left[1 - \frac{a\phi_2}{2} \int_1^\infty f(\beta) H(a\beta) d\beta \right]^2. \tag{4.37}$$

Here $H(a\beta)$ is the probability density of spheres with nearest neighbor at the distance $2a\beta$. Note that Eq. (4.37) is a two-point upper bound.

F. Evaluation of security-spheres upper bounds

1. Simple cubic lattice

As the first special case we consider evaluating the security-spheres upper bound for a simple cubic lattice with a lattice spacing of $2a\beta$. Then $\phi_2 = \pi/(6\beta^3)$ and Eq. (4.34) gives,

$$\frac{k}{k_s} \leq \frac{d(\beta)}{[1-(\phi_2/2)f(\beta)]^2}. \tag{4.38}$$

For small sink concentrations, Eq. (4.38) yields

$$\frac{k}{k_s} \leq 1 + \left[1+\frac{\pi}{6}\right]\left(\frac{6}{\pi}\right)^{1/3}\phi_2^{1/3} + O(\phi_2^{2/3}) \cong 1 + 1.8903\phi_2^{1/3} + O(\phi_2^{2/3}). \tag{4.39}$$

This upper bound is of the same form as the exact low concentration result of Felderhof.[5] His coefficient is 1.76, so Eq. (4.39) does indeed give an upper bound. We also compare Eq. (4.38) to the exact result for all volume fractions[5] in Fig. 4. For small ϕ_2, the bound is very sharp; the bound becomes poorer as ϕ_2 increases.

2. Random distribution of spheres

Next we consider a random distribution of equisized spheres of radius a. We see from Eq. (4.35) that $d(\beta)$ has a simple pole at $\beta = 1$. Therefore, in general, the integral in the numerator of Eq. (4.37) diverges and yields the trivial upper bound $k \leq \infty$. If $H(\beta)$ vanishes as $(\beta-1)^\epsilon$ at $\beta = 1$, where $\epsilon > 0$, the integral involving $d(\beta)$ converges and Eq. (4.37) gives a finite, positive upper bound on k [assuming the integral in the denominator of Eq. (4.37) is always less than or equal to $2/a\phi_2$]. We shall only treat such $H(\beta)$.

Consider now the case of low concentration and choose for $H(a\beta)$ the function[25]

$$H(a\beta) = \begin{cases} 0, & \beta < \beta_0 \\ \dfrac{12\phi_2\beta^2 e^{-4\phi_2(\beta^3-\beta_0^3)}}{a}, & \beta > \beta_0 \end{cases}. \tag{4.40}$$

When the dimensionless cutoff distance β_0 is zero, $H(a\beta)$ is the nearest neighbor probability density for independently uniformly distributed points with number density ρ. Substituting Eq. (4.40) into Eq. (4.37) yields

$$k/k_s \leq 1 + 3.42\phi_2^{1/3} + O(\phi_2^{2/3}). \tag{4.41}$$

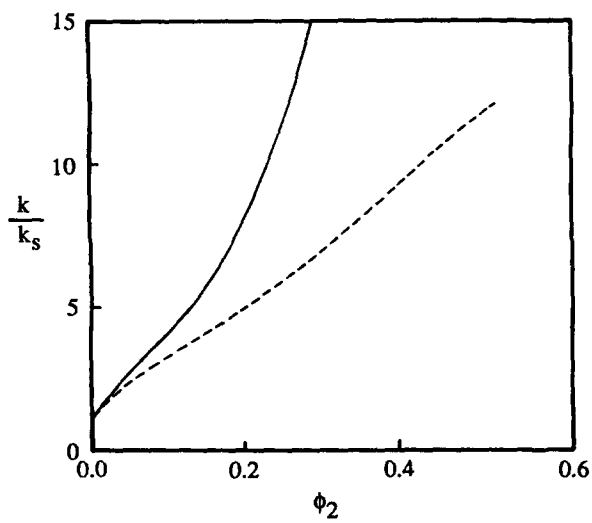

FIG. 4. The reduced rate constant k/k_s for a simple cubic array of spherical sinks vs ϕ_2. The dashed line (---) is the numerical result of Felderhof (Ref. 5) and the solid line (—) is our two-point upper bound (4.38).

It is helpful here to restate the three-point multiple-scattering lower bound for the case $\lambda = 1$ obtained in the previous subsection:

$$k/k_s \geq 1 + 5.56\phi_2 + O(\phi_2^2). \tag{4.42}$$

For $\phi_2 = 0.01$, the two-point upper bound (4.41) gives $k/k_s \leq 1.73$ and the three-point lower bound yields $k/k_s \geq 1.06$, this is to be contrasted with the expansion (4.14) which predicts $k/k_s = 1.20$. Therefore, for small ϕ_2, the lower bound gives the better estimate of k for a random distribution of impenetrable spherical sinks.

Finally, we remark that in a future work we shall compute upper bound (4.37) for a random distribution of spheres of arbitrary concentration using an appropriate nearest-neighbor probability density $H(a\beta)$.

V. DISCUSSION

A. Relationship to previous work on bounds

Reck and Prager[11] were the first to formulate variational principles for the upper and lower bounds on the rate constant. Using these variational principles, they derived a three-point lower bound and a two-point upper bound on k. The present work differs in several important ways. First of all, the effective equation which defines k, Eq. (2.12), is derived here using the method of homogenization. Reck and Prager, on the other hand, assume the existence of such a relation. Secondly, both our variational lower bounds, (3.5) and (3.17), and upper bounds, (3.8) and (3.19), are obtained from the same starting point, namely, Proposition 1, Eq. (2.15). Two different starting points were employed by Reck and Prager to derive their variational principles for bounds on k. Thirdly, Reck and Prager use a volume-average approach, whereas we utilize both a volume-average and an ensemble-average approach. Although our variational principle for the volume-averaged upper bound, Eq. (3.19), is identical to their corresponding principle, the same is not true for the respective variational principles associated with the lower bounds. Referring to the expression describing the admissible fields u, Eq. (3.18), for the volume-averaged lower bound, we see that Reck and Prager correctly required that $\Delta u = -\gamma$ in $\mathscr{V}_1$ but did not include the condition that the normal derivative of u on the macroscopic boundary must be equal to zero. It is difficult to construct trial fields which satisfy the latter condition. The variational principle for the lower bound obtained here using the ensemble-average approach, Eq. (3.5), has the advantage that this condition does not have to be satisfied. To our knowledge, the present formulation in terms of ensemble averages is new. Lastly, the trial fields employed in the present paper are different than the ones employed by Reck and Prager and hence all of the bounds derived in Sec. IV [except for Eq. (4.10)] are entirely new.

B. Comparison of the interfacial-surface and multiple-scattering lower bounds

We first observe an interesting relation between the interfacial-surface trial field Eq. (4.1) and the multiple-scattering trial field Eq. (4.15). Consider a distribution of N

totally impenetrable spheres ($\lambda = 1$), and restrict $u_1(\mathbf{y},\omega)$ to $\mathbf{y} \in \mathscr{V}_1$. Then, $\xi(\mathbf{x}) = \phi_1/s$ implies

$$u_1(\mathbf{y},\omega) = \gamma \left[\int_{\mathscr{V}_1} G(\mathbf{y}-\mathbf{x})d\mathbf{x} - \frac{\phi_1}{4\pi a^2 \rho} \int_{\partial\mathscr{V}} G(\mathbf{y}-\mathbf{x})d\mathbf{x} \right]$$

$$= \gamma \left[\int_{\mathscr{V}_1} G(\mathbf{y}-\mathbf{x})d\mathbf{x} - \frac{\phi_1}{\rho} \sum_{i=1}^{N} G(\mathbf{y}-\mathbf{r}_i) \right], \quad (5.1)$$

where we have used the mean-value theorem for harmonic functions. Equation (5.1) is strikingly similar (but *not* identical) to Eq. (4.15). The advantage of using Eq. (4.1) and not Eq. (4.15) is obvious when there is a large degree of penetrability (small λ), since the union of N nonoverlapping sphere surfaces does not represent the surface of the medium $\partial\mathscr{V}$ well in such instances. This explains why, for example, the three-point multiple scattering bound (4.29) is poorer than the two-point interfacial bound (4.10) for $\lambda = 0$ (cf. Fig. 3). Therefore, bounds which incorporate a certain level of information on the medium are not always necessarily sharper than bounds which involve less microstructural information. Nonetheless, within a certain class of trial fields (interfacial-surface fields, multiple-scattering fields, security-spheres fields, etc.), increasing the level of information leads to improved bounds. As the degree of impenetrability increases, the union of N nonoverlapping sphere surfaces, however, better represents the surface $\partial\mathscr{V}$. For large λ, therefore, the three-point multiple-scattering bound is superior to the two-point interfacial-surface bound because the former contains a greater amount of statistical information.

The interfacial-surface and multiple-scattering bounds have their own merits. The main advantage of the former is that it can be applied to media of arbitrary geometry (not just models such as distributions of spheres) and hence to "real" materials. On the other hand, the multiple-scattering bounds can be applied to any system composed of distributions of inclusions and can be systematically upgraded to include sophisticated multiple-scattering solutions.

ACKNOWLEDGMENTS

S. Torquato gratefully acknowledges the support of the Office of Basic Energy Sciences, U. S. Department of Energy, under Grant No. DE-FG05-86ER 13482. J. Rubinstein was supported by the National Science Foundation and by the Office of Naval Research. The authors are thankful to J. D. Beasley for a critical reading of this manuscript.

[1] D. F. Calef and J. M. Deutch, Annu. Rev. Phys. Chem. **34**, 493 (1983).
[2] M. Smoluchowski, Phys. Z. **17**, 557 (1916).
[3] B. U. Felderhof and J. M. Deutch, J. Chem. Phys. **64**, 4551 (1976).
[4] K. Mattern and B. U. Felderhof, Physica A **143**, 1 (1987).
[5] B. U. Felderhof, Physica A **130**, 34 (1985).
[6] M. Muthukumar, J. Chem. Phys. **76**, 2667 (1982).
[7] R. I. Cukier and K. F. Freed, J. Chem. Phys. **78**, 2573 (1983).
[8] M. Fixman, J. Chem. Phys. **81**, 3666 (1984).
[9] K. Mattern and B. U. Felderhof, Physica A **143**, 21 (1987).
[10] P. M. Richards, J. Chem. Phys. **85**, 3520 (1986); P. M. Richards, Phys. Rev. B **35**, 248 (1987).
[11] R. A. Reck and S. Prager, J. Chem. Phys. **42**, 3027 (1965).
[12] M. Doi, J. Phys. Soc. Jpn. **40**, 567 (1976).
[13] S. Torquato, J. Appl. Phys. **58**, 3790 (1985); S. Torquato and F. Lado, Phys. Rev. B **33**, 6428 (1986).
[14] S. Torquato, J. Stat. Phys. **45**, 843 (1986).
[15] S. Prager, Phys. Fluids **4**, 1477 (1961); H. L. Weissberg and S. Prager, Phys. Fluids **5**, 1390 (1962); S. Prager, Physica **29**, (1963); H. L. Weissberg and S. Prager, Phys. Fluids **13**, 2958 (1970).
[16] G. C. Papanicolaou and S. R. S. Varadhan, in *Colloquia Mathematica Societatis Jânos Bolyai* (North-Holland, Amsterdam, 1982), pp. 835–873.
[17] The definition (2.12), unlike other definitions (cf. Refs. 11 and 12), includes the constant diffusion coefficient D. Specifically, the definition of Refs. 11 and 12 is scaled by a factor D.
[18] L. Blum and G. Stell, J. Chem. Phys. 71, **42** (1979); J. J. Salacuse and G. Stell, *ibid.* **77**, 2071 (1982).
[19] S. Torquato, J. Chem. Phys. **81**, 5079 (1984).
[20] S. Torquato, J. Chem. Phys. **85**, 7178 (1986).
[21] Note that the definition of k used in Ref. 20 differed from the present definition by a factor involving ϕ_1. See: P. M. Richards and S. Torquato, J. Chem. Phys. **87**, 4612 (1987), for a clarification of this point.
[22] S. Torquato, J. Chem. Phys. **84**, 6345 (1986).
[23] S. Torquato and J. D. Beasley, Phys. Fluids **30**, 633 (1987); J. Rubinstein and S. Torquato (to be published).
[24] J. B. Keller, L. A. Rubenfeld, and J. E. Molyneux, J. Fluid Mech. **30**, 97 (1967).
[25] J. Rubinstein and J. B. Keller, Phys. Fluids **30**, 2919 (1987).